

# Corner stress fields in sliding at high friction coefficients

Kisik Hong<sup>a</sup>, Wei Lu<sup>a</sup>, M.D.Thouless<sup>a,b</sup>, J.R.Barber<sup>a</sup>

<sup>a</sup>*Department of Mechanical Engineering, University of Michigan, Ann Arbor, MI 48109-2125, U.S.A.*

<sup>b</sup>*Department of Materials Science and Engineering, University of Michigan, Ann Arbor, MI 48109-2136, U.S.A.*

---

## Abstract

If an elastic body with a sharp corner slides over an elastic half-plane, the stress and displacement fields near the corner can be characterized by the leading term in an asymptotic [eigenfunction] series. However, there exists a critical friction coefficient  $f = f_d$  at which an infinitesimal increase in  $f$  appears to imply a discontinuous change from singular to bounded local fields at the leading edge. Here, we show that this conclusion is incorrect. Instead, the contact region shrinks to zero at  $f = f_d$  implying the existence of a concentrated contact force, but the singular field associated with point contact is retained for  $f > f_d$ . We also show that a non-linear solution using a Generalized Neo-Hookean constitutive law gives the same conclusion, and that the concentrated force generated is well predicted by the linear analysis. However, in contrast to the linear solution, the total strain energy in the non-linear solution is bounded.

*Keywords:* asymptotic stress field; sliding; friction; concentrated force.

---

## 1. Introduction

If an elastic body with a sharp corner is pressed against an elastic half-plane as shown in Fig. 1, the stress field near the corner can be expanded as an asymptotic series of the form

$$\sigma_{ij}(r, \theta) = \sum_{n=1}^{\infty} K_n r^{\lambda_n - 1} f_{ij}^n(\theta) \quad (1)$$

[1, 2], where  $\lambda_n$  and  $f_{ij}^n(\theta)$  are eigenvalues and eigenfunctions respectively,  $(r, \theta)$  are polar coordinates centered on the corner, and  $K_n$  are a set of coefficients depending on the far-field loading. The eigenvalues are generally arranged in order of ascending real

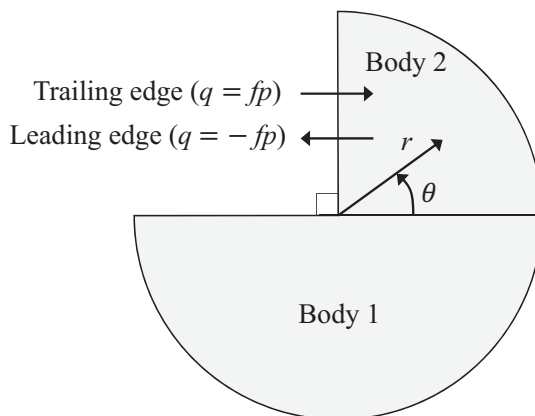


Figure 1: A quarter-plane indenting a half-plane. At a trailing edge [body 2 slipping relatively to the right],  $q = fp$  and at a leading edge [body 2 slipping relatively to the left],  $q = -fp$ .

part, so the local stress field close to the corner is dominated by the first term of equation (1). In particular, if the field is singular, the strength of the singularity is determined by  $\lambda_1$  and  $K_1$  plays the rôle of a generalized stress-intensity factor.

If the upper body (2) in Fig. 1 slides over the lower body (1), and if Amontons' friction law is assumed, the local contact pressure  $p(r)$  and the shear traction  $q(r)$  must satisfy the condition  $q = \pm fp$ , where the sign depends on the direction of sliding. Here, the sign is positive when body 2 slides to the right [trailing-edge slip] and negative when it slides to the left [leading-edge slip]. It is then convenient to normalize the first term of equation (1) in the form

$$p(r) \approx -K_1 r^{\lambda_1 - 1}; \quad q(r) \approx \pm f K_1 r^{\lambda_1 - 1}. \quad (2)$$

Karuppanan *et al.* [3] studied the case where body 2 has a right-angle corner and the two bodies are of similar materials. The first two eigenvalues are shown as a function of  $f$  in Fig. 2. These comprise a complex-conjugate pair for trailing-edge slip with  $f > f_c$ , but these bifurcate into two distinct real eigenvalues for  $f < f_c$ , including negative values corresponding to leading-edge slip.

Notice, in particular, that in leading-edge slip, the lowest eigenvalue decreases with increasing  $f$  and goes to zero at  $f = f_d = 2.04$ . Energetic considerations restrict the eigenvalues to the range  $\Re(\lambda_n) > 0$  for all  $n$ , so conventional wisdom would say that for  $f > f_d$ , the corner field would be determined by the first positive eigenvalue, implying bounded stresses at the corner. However, this implies a discontinuous change in leading-

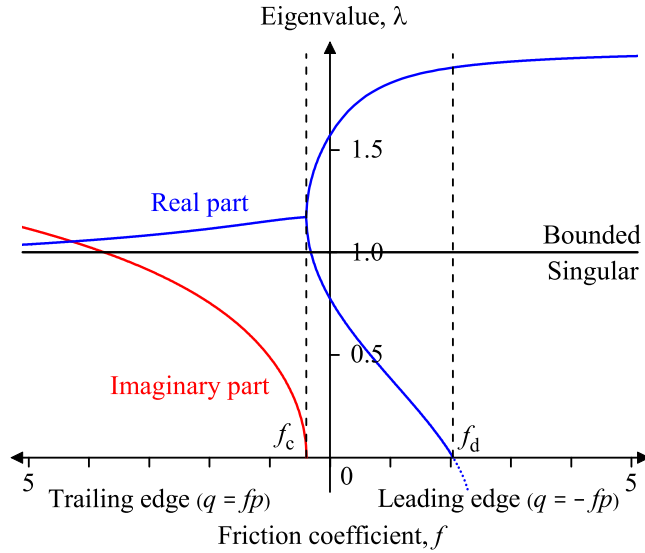


Figure 2: Slip eigenvalues as a function of friction coefficient for the contact between elastically similar materials.

edge behaviour over an infinitesimal change of friction coefficient near  $f = f_d$ , which seems counter-intuitive. This is the question which we explore in the present paper.

Of course, coefficients of friction in this range are rare, so the question might be deemed rather academic, but we would like to know the answer in the interests of mathematical completeness. Also, we shall show that with dissimilar materials the same effect can occur with coefficients as low as 1.57, and there do exist material combinations where such values are obtainable. For example, the coefficient of friction between a  $\text{UO}_2$  fuel pellet and Zircaloy cladding under irradiation can be as large as 3 depending on the operating condition [4, 5]. Also, rubbers in contact with other materials, such as glass or silicon carbide, can yield coefficients larger than 2 [6].

## 2. A finite-element model

To explore this question in more detail, we developed a finite-element model of the system shown in Fig. 3, in which a rectangular strip is pressed against a body with a plane surface by a uniform pressure  $p$  applied to the upper edge. This edge was also subjected to a small uniform leftward displacement  $d$  sufficient to ensure slip at all contact nodes,

Refined mesh near the corner

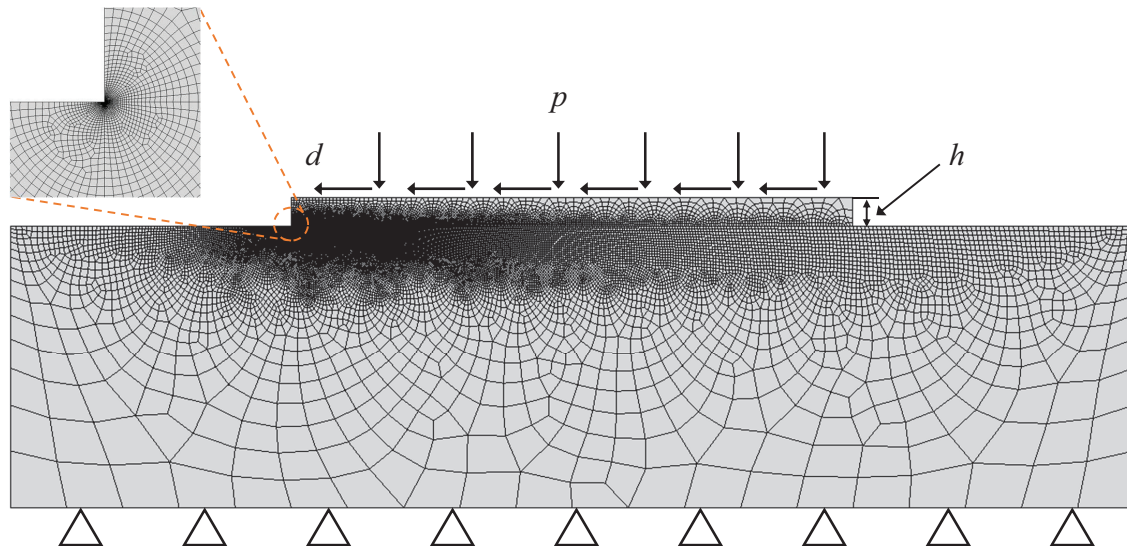


Figure 3: Plane-strain finite-element model to evaluate the asymptotic behaviour at the leading edge (left-hand corner).

since the alternative imposition of shear traction boundary conditions would leave a rigid-body degree of freedom. Hard contact boundary conditions were used at the interface with the direct method to ensure no interpenetration, and a classical Coulomb model was implemented for the tangential behavior, using the augmented-Lagrangian method. Initially, following Karuppanan *et al.* [3], we used similar elastic properties for the two bodies, but later we shall report results for the more general case.

Since we are interested specifically in the leading-edge behaviour, we refined the mesh near the left-hand corner. The adequacy of this mesh refinement was tested by comparing the strength of the stress singularity  $[\lambda_1 - 1]$  from the asymptotic analysis with the slope of a log-log plot of the finite-element stresses along the interface for  $f < f_d$ . Good agreement was obtained when the ratio of the smallest elements to the height of body 2 [the smallest linear dimension of the object] was set to be 0.001.

### 2.1. Results for $f \leq f_d$

The finite-element results show that there exists a critical friction coefficient  $f_e$  such that for  $f_e < f < f_d$ , an interior separation region  $a < r < b$  develops adjacent to the slip region at the corner, as shown in Fig. 4. For similar materials  $f_e = 1.66$  and  $f_d = 2.04$ .

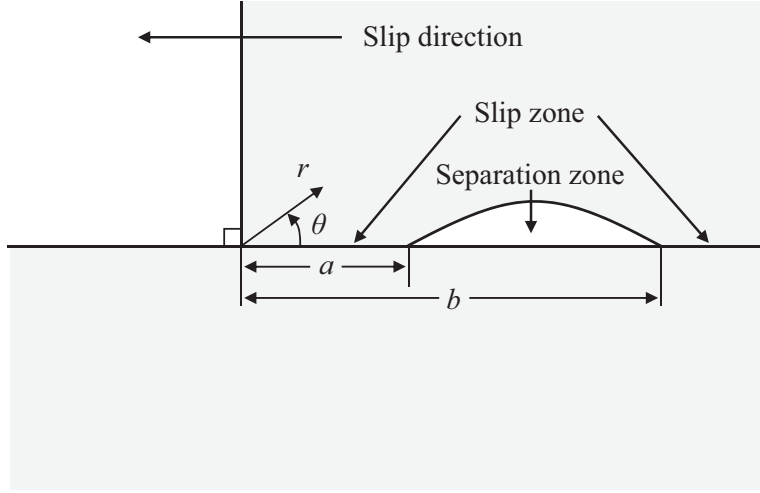


Figure 4: Slip and separation zones developed at the leading edge for  $f_e < f < f_d$

For a given value of  $f$  in this range, the dimensions  $a, b$  scale with the height  $h$  of the upper body, showing that these features are determined by the macroscopic dimensions and loading of the system. In other words, there is no inherent length scale in the asymptotic field.

As  $f \rightarrow f_d$ ,  $a \rightarrow 0$ , whereas  $b$  tends to a non-zero constant depending on the macroscopic conditions. Thus, in the limit  $f = f_d$  we essentially have a point contact at the corner. This is of course consistent with an eigenvalue of zero, since the stress field is then proportional to  $r^{-1}$  as in the classical Flamant solution.

To ensure that this point contact is not an artifact of the necessarily finite mesh size, a technique was developed which enables us to obtain results for a highly refined mesh, which in the original model would lead to a very large ratio between the dimensions of the largest and smallest elements. The procedure is as follows:-

1. Run the simulation with the original model as in Fig. 5 (right).
2. Consider a small circular region centered on the corner and capture the stress or displacement field  $[\sigma \text{ or } u]$  along the circular boundary.
3. Build a new model comprising only the circular region, and apply the obtained field along the boundary as in Fig. 5 (left).

This procedure can be repeated if necessary to achieve any desired level of mesh refinement in the corner. In the present case, we used it to obtain results for a corner

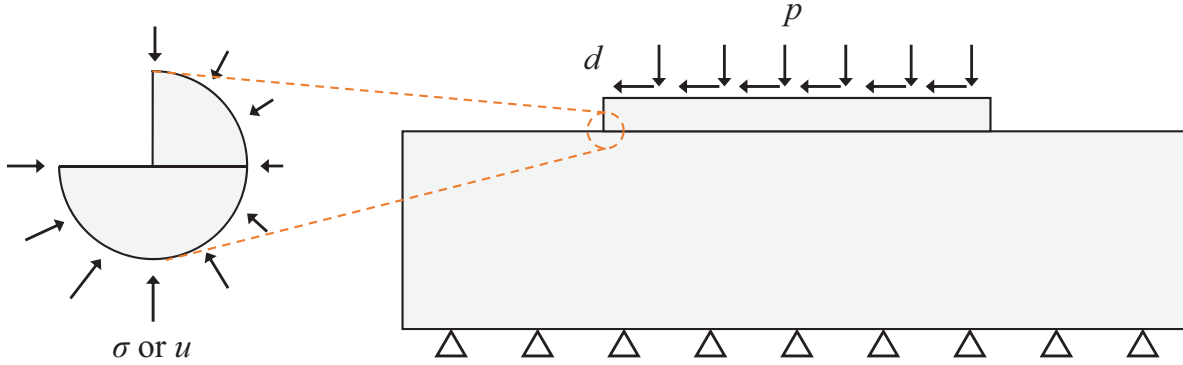


Figure 5: Schematic of a finite-element simulation technique to implement a highly refined mesh near the corner of interest.

element dimension of  $10^{-10}h$ , for which we still obtained only a single node in contact at  $f = f_d$ . Also, with each level of refinement, the tractions and displacements on the circular boundary approached more closely to the sinusoidal asymptotic form, and the concentrated force on the corner node was insensitive to mesh refinement beyond that used in the original model.

## 2.2. Results for $f > f_d$

We next conducted simulations to investigate the leading-edge behaviour for  $f > f_d$ , for which a conventional asymptotic argument based on Fig. 2 would predict bounded stresses in the corner. Instead, we once again obtained single-node [point] contact at the corner with an adjacent separation zone. Also, the magnitude of this force and the size of the separation zone increase with increasing  $f$ , for given macroscopic geometry and loading conditions.

This raises the question “Why does the system not follow the asymptotic form suggested by Fig. 2 for  $f > f_d$ ?” To answer this, we must remember that the first term in an asymptotic series is a good approximation to the actual field only at values of  $r$  that are small compared with the other dimensions in the contact geometry. In other words, there must exist a ‘ $K_1$ -dominated region’. Now Fig. 2 is based on the assumption that we have contact with slip adjacent to the corner, so a  $K_1$ -dominated region [ $r \ll a$ ] can be found for the configuration of Fig. 4 if and only if the extent of the leading slip zone  $a > 0$ . If we have point contact at the corner [ $a = 0$ ], no such region exists. It is of course possible to develop an alternative asymptotic solution for the case where a slipping point contact at the corner abuts a separation zone, but unsurprisingly this would yield stresses varying

with  $r^{-1}$ , corresponding to  $\lambda_1 = 0$ .

### 2.3. A hyperelastic solution

Point contacts and the associated asymptotic fields are strictly inadmissible in linear elasticity, since the strain energy in a small circular region surrounding the singular point is then logarithmically unbounded. Also, the displacement field is logarithmically unbounded in the corner, which is reflected in the finite-element solution by corner displacements that continue to increase as the mesh is refined, even though the stress field converges.

Clearly the assumptions of linear elasticity will break down sufficiently near the corner [this is true even for admissible singularities] due to non-linearities in the kinematics and possibly also in the constitutive law, and it is natural to expect these effects to distribute the concentrated force over a finite contact region. Since the mathematical objection to the linear elastic solution is associated with unbounded strain energy, we chose to explore the non-linear solution using a hyperelastic model, since in this context, energy is still conserved. For a hyperelastic material, the strain energy density is defined as a function of the invariants of the deformation tensor. In this analysis, we used the Generalized Neo-Hookean model [7] which incorporates a range of ‘hardening’ characteristics, represented by an exponent  $n$  [ $> 1/2$ ], in the Neo-Hookean model [for which  $n = 1$ ]. The effect of  $n$  is to change the rate of strain hardening in response to uniaxial tension [8].

Surprisingly [at least to the present authors], the non-linear results continue to show contact at a single node at the corner. Also, the contact force remains essentially constant with mesh refinement, with a value that is only slightly [less than 1%] lower than that of the linear solution. This implies, incidentally, that a good approximation to the non-linear solution could be obtained by using the two-stage procedure of Fig. 5, where the simpler linear solution is used for the first [coarse mesh] step. More generally, the non-linear solution of Fig. 5 (left) could be patched into the corner field of any linear contact problem exhibiting a concentrated corner force.

#### 2.3.1. Energetic considerations

Equilibrium arguments show that the components of the Cauchy stress due to a concentrated force must still vary with  $r^{-1}$ , but in contrast to linear elasticity, this singularity is physically admissible in the framework of nonlinear elasticity and indeed has been reported in hyperelastic problems involving cracks [9, 10]. If the local stress components vary with  $r^{-1}$ , the corresponding displacements have the form  $r^{1-1/(2n)}$ , and are therefore

bounded as  $r \rightarrow 0$ . The strain energy density then involves an  $r^{-1}$  singularity, and hence the total strain energy in a small circle surrounding the singular point is also bounded.

### 3. Dissimilar materials

If the materials of the two bodies are different, the eigenvalues  $\lambda_n$  of equation (1) during sliding satisfy the equation

$$(1 + \alpha) \cos(\lambda\pi) \left[ \sin^2 \left( \frac{\lambda\pi}{2} \right) - \lambda^2 \right] + \frac{1 - \alpha}{2} \sin^2(\lambda\pi) \pm f \sin(\lambda\pi) \left\{ (1 - \alpha)\lambda(1 + \lambda) - 2\beta \left[ \sin^2 \left( \frac{\lambda\pi}{2} \right) - \lambda^2 \right] \right\} = 0 \quad (3)$$

[11, 12], where  $\alpha, \beta$  are Dundurs' bimaterial parameters [13], and as before we take the negative sign for leading-edge slip. Equation (3) has a trivial root  $\lambda = 0$  for all  $\alpha, \beta, f$ , so to determine the critical coefficient of friction  $f_d$ , we use L'Hôpital's rule to determine the condition for there to be a second non-trivial root. We obtain

$$f_d = \frac{\pi}{2} - \frac{\pi^2 - 4}{4\pi} \left( \frac{\alpha + 1}{\alpha - 1} \right) = \frac{\pi}{2} + \frac{\pi^2 - 4}{4\pi} \left( \frac{1 - \nu_1}{1 - \nu_2} \right) \frac{G_2}{G_1}, \quad (4)$$

where  $G_i, \nu_i$  are respectively the shear modulus and Poisson's ratio for body  $i$ . The minimum value is  $f_d = 1.57$ , which occurs when  $\alpha = -1$ , or  $G_2/G_1 \rightarrow 0$  — i.e. when the half-plane (1) has a much larger elastic modulus than the body with the corner (2).

### 4. Conclusions

We have shown that if an elastic body with a right-angle corner slides over an elastic half-plane, there exists a critical coefficient of friction  $f_d$  above which a concentrated point contact occurs at the leading edge, with an adjacent separation region. This appears to contradict the asymptotic analysis of Karuppanan *et al.* [3] which predicts a bounded asymptotic field for  $f > f_d$ , but this result depends on the existence of a  $K_1$ -dominated slip region which does not exist if contact occurs only at a point.

In linear elasticity, the corresponding  $1/r$  singularity implies infinite strain energy in a finite corner region and hence is strictly inadmissible. However, we show that a hyperelastic solution of the problem resolves this issue and also predicts a concentrated corner force whose magnitude is almost identical to that in the linear solution.



## References

- [1] M. L. Williams, “Stress singularities resulting from various boundary conditions in angular corners of plates in extension,” *J. Appl. Mech.*, vol. 19, no. 4, pp. 526–528, 1952.
- [2] D. B. Bogy, “Edge-bonded dissimilar orthogonal elastic wedges under normal and shear loading,” *J. Appl. Mech.*, vol. 35, no. 3, pp. 460–466, 1968.
- [3] S. Karuppanan, C. M. Churchman, D. A. Hills, and E. Giner, “Sliding frictional contact between a square block and an elastically similar half-plane,” *Eur. J. Mech.*, vol. 27, no. 3, pp. 443–459, 2008.
- [4] Y. V. Bozhko, A. M. Bolobolichiev, A. V. Kostochka, and V. M. Shchavelin, “Coefficient of static friction of the uranium dioxide-zirconium alloy pair under irradiation,” *Soviet Atomic Energy*, vol. 71, no. 5, pp. 945–948, 1991.
- [5] V. M. Shchavelin, A. V. Kostochka, A. A. Kuznetsov, I. S. Golovnin, and Y. K. Bibilashvili, “In-reactor study of the friction characteristics of reactor materials,” *Soviet Atomic Energy*, vol. 61, no. 3, pp. 686–690, 1986.
- [6] K. A. Grosch, “The relation between the friction and visco-elastic properties of rubber,” *Proc. R. Soc. Lond. A*, vol. 274, no. 1356, pp. 21–39, 1963.
- [7] J. K. Knowles, “The finite anti-plane shear field near the tip of a crack for a class of incompressible elastic solids,” *Int. J. Fract.*, vol. 13, no. 5, pp. 611–639, 1977.
- [8] P. H. Geubelle and W. G. Knauss, “Finite strains at the tip of a crack in a sheet of hyperelastic material: I. Homogeneous case,” *J. Elast.*, vol. 35, no. 1–3, pp. 61–98, 1994.
- [9] J. K. Knowles and E. Sternberg, “Large deformations near a tip of an interface-crack between two Neo-Hookean sheets,” *J. Elast.*, vol. 13, no. 3, pp. 257–293, 1983.
- [10] P. H. Geubelle, “Finite deformation effects in homogeneous and interfacial fracture,” *Int. J. Solid Struct.*, vol. 32, no. 6–7, pp. 1003–1016, 1995.
- [11] E. E. Gdoutos and P. S. Theocaris, “Stress concentrations at the apex of a plane indenter acting on an elastic half-plane,” *J. Appl. Mech.*, vol. 42, no. 3, pp. 688–692, 1975.

- [12] M. Comninou, "Stress singularity at a sharp edge in contact problems with friction," *Zeitschrift für Angew. Math. und Phys. ZAMP*, vol. 27, no. 4, pp. 493–499, 1976.
- [13] J. Dundurs, "Discussion on Edge-bonded dissimilar orthogonal elastic wedges under normal and shear loading," *J. Appl. Mech.*, vol. 36, no. 3, pp. 650–652, 1969.